Experiments with γ detectors at LEPS2

H. Shimizu

Laboratory of Nuclear Science

Tohoku University

LEPS2 Workshop, RCNP, Jan 8-9, 2007

Diversity of Hadron Physics

confinement

phase transitions
confinement
=> deconfinement
phase at high T
HI beam

chiral symmetry

precursors to
chiral transition
in nuclei
γ beam
hadron beam

QCD

Hadron Physics
research

in free space

in nuclear matter

spectroscopy
the most basic study

New LEPS beam will give a new approach.

Some physics to be discussed in the LEPS2 project

1) Hadrons under χS

* meson sector

(a) study of Namb-Goldstone bosons in free space

(b) partial restoration of χS in nuclei $\Rightarrow$ softening of σ

(c) $U_A(1)$ anomaly

$U_A(1)$ restoration? <= χS restoration (experiments)

* baryon sector (N*: negative parity baryon)

2 kinds of χ transformations

2) Hadrons and exotics

* pentaquark baryons

Θ^+ and others in the anti-decuplet

* dibaryon ($I,J^{PC}=0,0^-$)

3) QED higher order effects (measurement of birefringence)

* direct measurement of the vacuum polarization

Hadrons under chiral symmetry

* Meson sector

(a) σ in free space

$\sigma \to 2\gamma$ (BR~10^{-5})

(b) Partial restoration of χS in nuclei

++ softening of σ

$\sigma \to 2\gamma$

$\sigma \to 2\pi^0$

(c) Study of Namb-Goldstone bosons

++ measurements of π^0 polarizabilities

++ transition form factors of η

(d) $U_A(1)$ problem

"Does χS restoration affect the $U_A(1)$ problem?"

++ $\eta' \to 2\gamma$ in nuclei

experiments with γ detectors

Pion Polarizabilities

- Electromagnetic polarizabilities of a meson M:
The polarizabilities α_M and β_M measure the induced meson dipole moments

$$\begin{cases} \boldsymbol{d} = \alpha_M \boldsymbol{E} \\ \boldsymbol{m} = \beta_M \boldsymbol{B} \end{cases} \quad (1)$$

in an external field $\boldsymbol{E}$ and $\boldsymbol{B}$.

a reflection of
the internal structure
of the particle

one of the most fundamental
properties of the particle

- How to measure the polarizabilities:

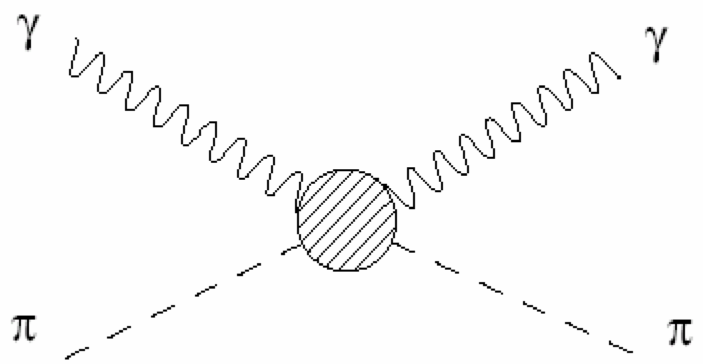

Compton amplitude at low energies

$$T(\gamma\pi \to \gamma\pi) = -2e^2(\boldsymbol{\epsilon}_1 \cdot \boldsymbol{\epsilon}_2) + 2m[\alpha_\pi \omega_1 \omega_2 (\boldsymbol{\epsilon}_1 \cdot \boldsymbol{\epsilon}_2) + \beta_\pi (\boldsymbol{\epsilon}_1 \times \boldsymbol{k}_1) \cdot (\boldsymbol{\epsilon}_2 \times \boldsymbol{k}_2)] \quad (2)$$

Measurements for polarizabilities of charged pions

1) radiative π-Z scattering

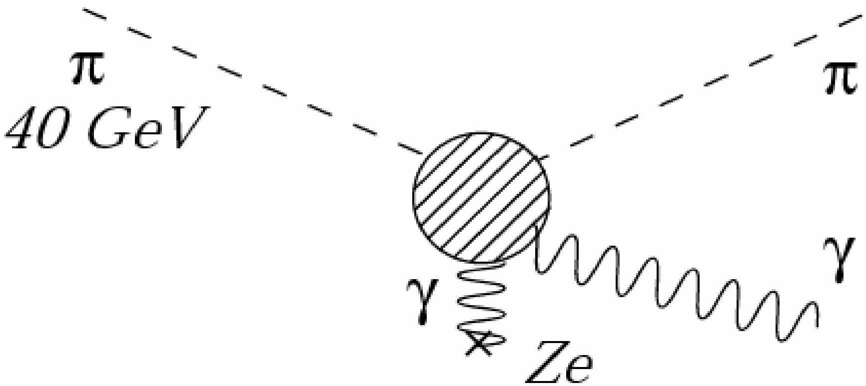

Serpukhov

2) π photoproduction

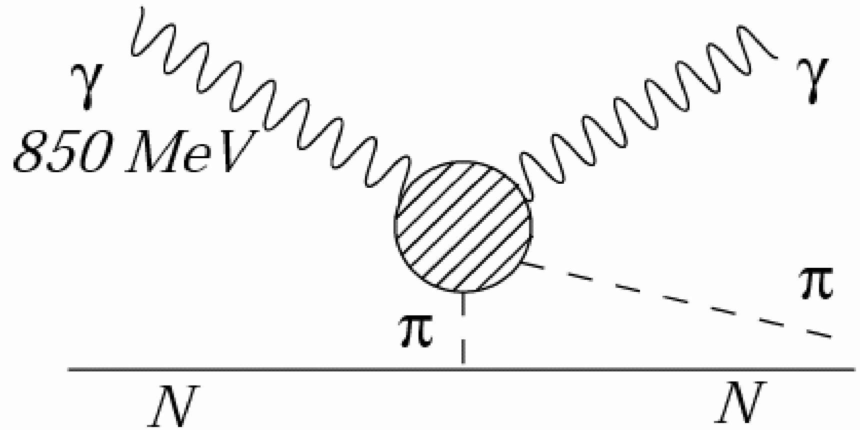

Lebedev

3) direct γγ→ππ process

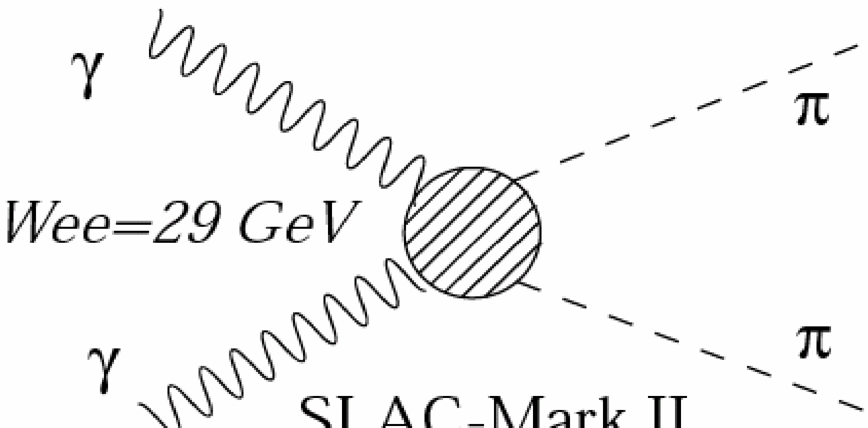

SLAC-Mark II
(π^0:DESY-Crystal Ball)

4) Primakov production

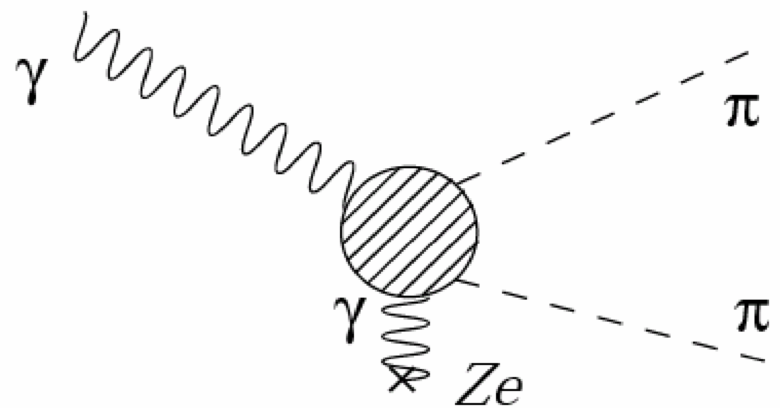

SPring-8/LEPS

Pion Polarizabilities

χPT $\alpha_{\pi\pm}/10^{-4}\ fm^3$
2.7 one-loop
2.2 two-loop

Table 1. The experimental data presently available for the pion polarizabilities.

Experiments		$\alpha_{\pi^\pm}/10^{-4}$ fm^3	$\alpha_{\pi^0}/10^{-4}$ fm^3
$\pi^- Z \to \gamma\pi^- Z$, Serpukhov (1983) [10]		$6.8 \pm 1.4 \pm 1.2$	
$\gamma p \to \gamma\pi^+ n$, Lebedev Phys. Inst. (1984) [11]		20 ± 12	
D. Babusci *et al.* (1992) [12]			
$\gamma\gamma \to \pi^+\pi^-$:	PLUTO (1984) [13]	$19.1 \pm 4.8 \pm 5.7$	
	DM 1 (1986) [14]	17.2 ± 4.6	
	DM 2 (1986) [15]	26.3 ± 7.4	
	MAPK II (1990) [16]	2.2 ± 1.6	
$\gamma\gamma \to \pi^0\pi^0$:	Crystal Ball (1990) [17]		$\pm 0.69 \pm 0.11$
F. Donoghue, B. Holstein (1993) [18]			
$\gamma\gamma \to \pi^+\pi^-$:	MARK II	2.7	
$\gamma\gamma \to \pi^0\pi^0$:	Crystal Ball		-0.5
		$(\alpha+\beta)_{\pi^0}/10^{-4}$ fm^3	$(\alpha-\beta)_{\pi^0}/10^{-4}$ fm^3
A. Kaloshin, V. Serebryakov (1994) [19]			
$\gamma\gamma \to \pi^0\pi^0$:	Crystal Ball	1.00 ± 0.05	-0.6 ± 1.8
L. Fil'kov, V. Kashevarov (1999) [6]			
$\gamma\gamma \to \pi^0\pi^0$:	Crystal Ball	0.98 ± 0.03	-1.6 ± 2.2

Mainz: $\gamma p \to \gamma\pi^+ n$ $\quad (\alpha-\beta)_{\pi^+} = (11.6 \pm 1.5 \pm 3.0 \pm 0.5)\times 10^{-4}\ fm^3$

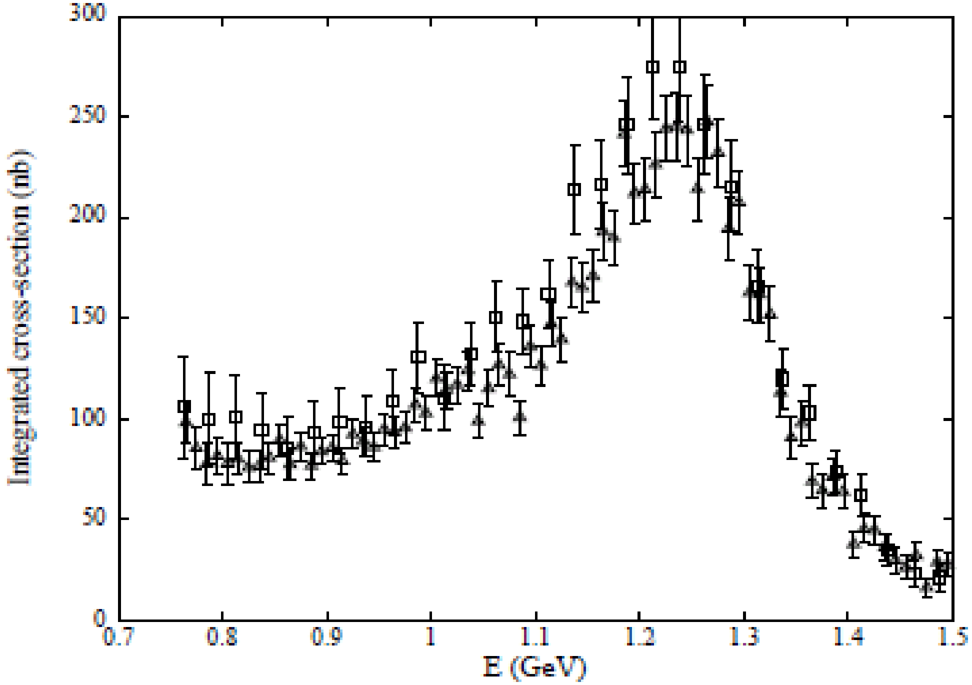

$$\gamma\gamma \rightarrow \pi^{+}\pi^{-}$$

Fig. 5. Comparison between Mark II [8] (diamonds) and CELLO [12] (squares) integrated cross-sections for $\gamma\gamma \rightarrow \pi^+\pi^-$ in their common energy range

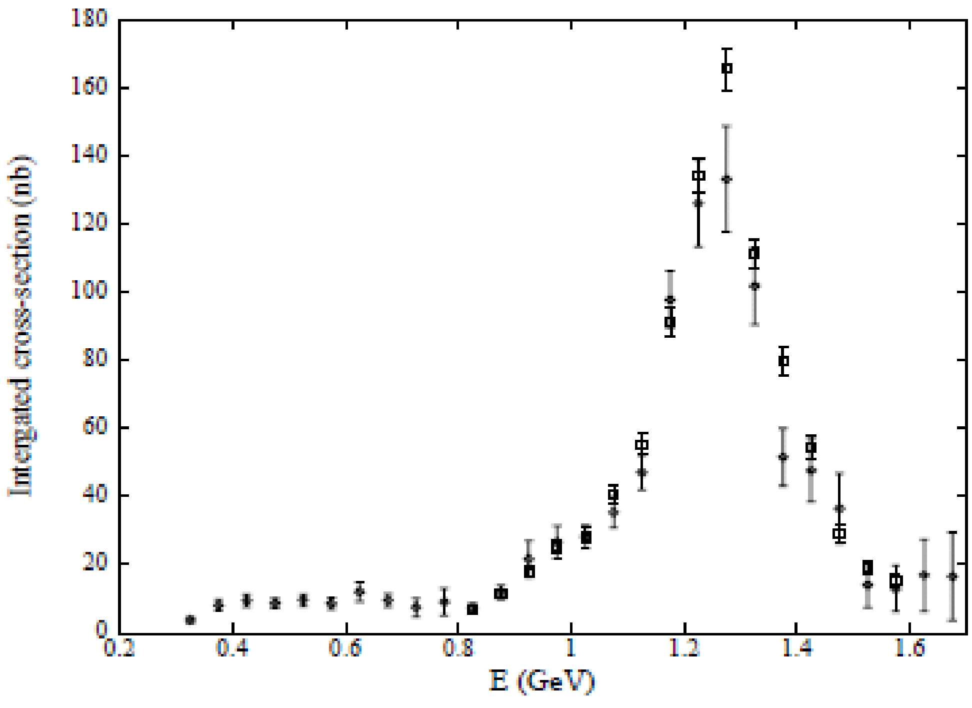

$$\gamma\gamma \rightarrow \pi^{0}\pi^{0}$$

Fig. 6. Comparison between CB88 [7] (diamonds) and CB92 [13] (squares) integrated cross-sections for $\gamma\gamma \rightarrow \pi^0\pi^0$

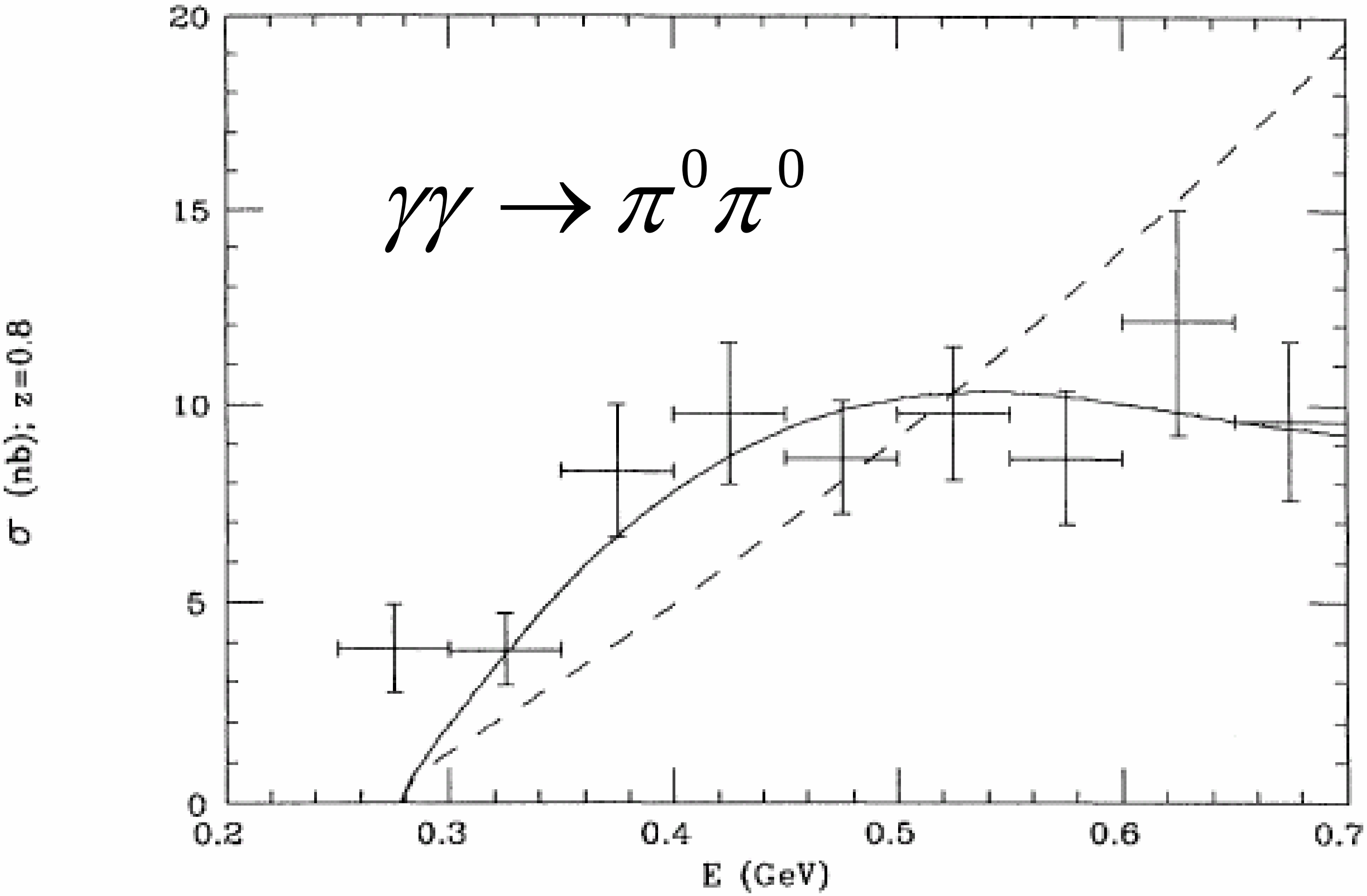

FIG. 2. The data points shown are the $\gamma\gamma \to \pi^0\pi^0$ cross section (with $|\cos\theta| < Z \equiv 0.8$) measured by the Crystal Ball Collaboration (Ref. [4]). The dashed curve is the prediction of one-loop chiral perturbation theory, while the solid curve is a full no-free-parameter dispersive calculation, as described in the text.

Donoghue and Holstein, PRD48(1993)137.

Measurements of polarizabilities of the neutral pion

1) radiative π-Z scattering

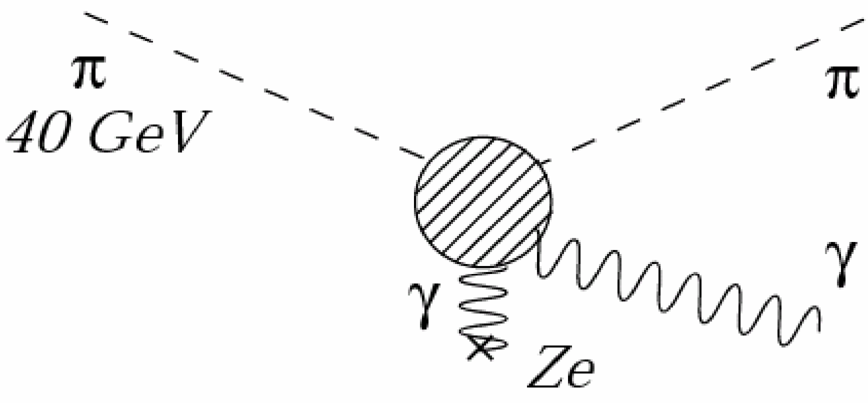

Serpukhov

2) π photoproduction

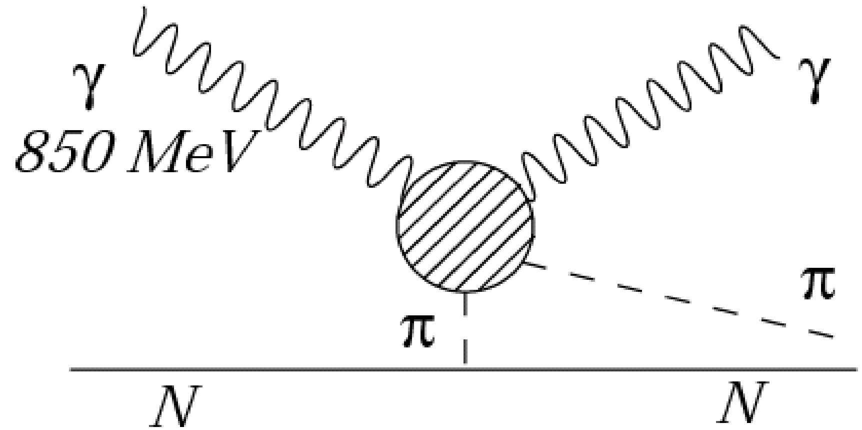

Lebedev

3) direct γγ→ππ process

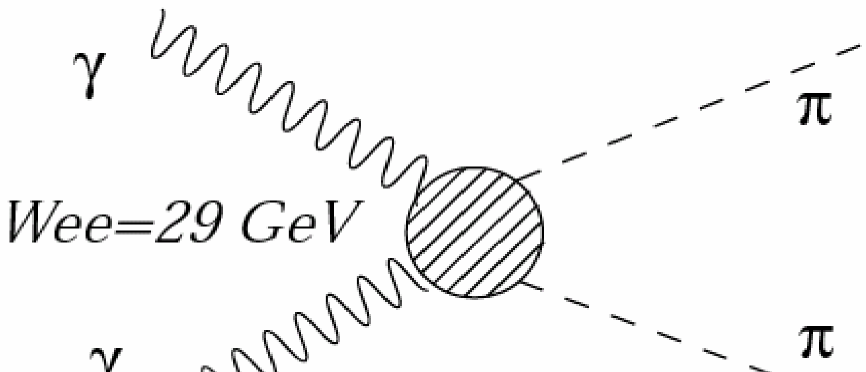

SLAC-Mark II
(π^0:DESY-Crystal Ball)

4) Primakov production

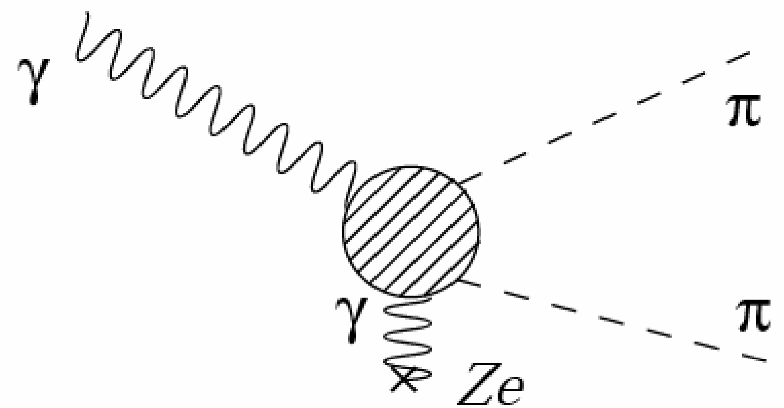

SPring-8/LEPS

Cross section for π0π0 photoproduction in the Coulomb field of the nucleus

$$\frac{d\sigma_C(\gamma A \to \pi\pi A)}{ds} = \frac{\alpha}{\pi} Z^2 \log\left(\frac{\sqrt{s}}{2m_\pi}\right)\frac{1}{s}\sigma^{\gamma\gamma\to\pi\pi}(s)$$

where $s = m_{\pi\pi}^2$

Belkov Dillig and Lanyov, J. Phys. G23(1997) 823.

$$\sigma^{\gamma\gamma\to\pi\pi}(s) = \int \frac{d\sigma(\gamma\gamma \to \pi^0\pi^0)}{d\Omega} d\Omega = \frac{\pi\alpha^2}{s}\sqrt{\frac{s-4m_\pi^2}{s}}\left|f_{\pi^0}(s)\right|^2$$

$$f_{\pi^0}(s) = \frac{m_\pi}{4\alpha}(\overline{\alpha}_{\pi^0} - \overline{\beta}_{\pi^0})s + O(s^2, sm_\pi^2)$$

Donoghue and Holstein, PRD48 (1993)197.

Hadrons under chiral symmetry

* Meson sector

(a) σ in free space

$\sigma \to 2\gamma$ (BR~10^{-5})

(b) Partial restoration of χS in nuclei

++ softening of σ

$\sigma \to 2\gamma$

$\sigma \to 2\pi^0$

(c) Study of Namb-Goldstone bosons

++ measurements of π^0 polarizabilities

++ transition form factors of η

(d) $U_A(1)$ problem

"Does χS restoration affect the $U_A(1)$ problem?"

++ $\eta' \to 2\gamma$ in nuclei

Mass spectrum of pseudoscalar mesons

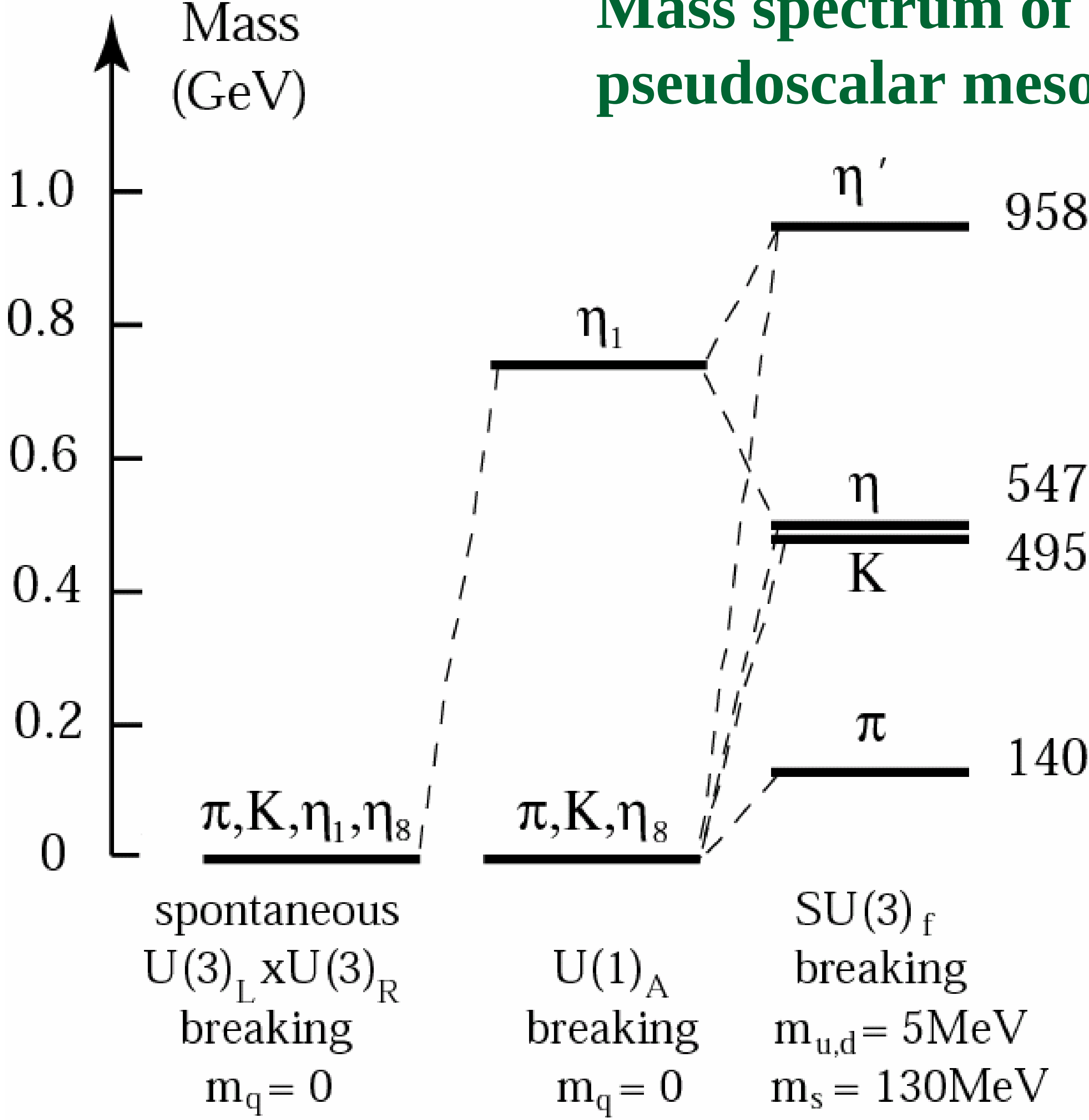

Whether axial U(1) anomaly is affected or not?

discussion
in detail
=> Takizawa

Does chiral restoration affect $U_A(1)$ restoration?

- Search for the effect in nuclei

  The η' meson is a good candidate.

- Particles decaying from η' have to be weak interacting ones in the final state.

- Plan to measure

  process $\eta' \rightarrow \gamma\gamma$ in nuclei

  η' at rest

  full width: Γ=0.2 MeV

  => $p_{\eta'} \leq 0.01 GeV/c$

  $\Leftrightarrow d \leq 10\, fm$

η' decay modes	**branching ratio**
$\eta' \rightarrow \pi^+\pi^-\eta$	44.3%
$\eta' \rightarrow \rho^0\gamma$	29.5%
$\eta' \rightarrow \pi^0\pi^0\eta$	20.9%
⋮	
$\eta' \rightarrow \gamma\gamma$	2.1%

γp total cross section

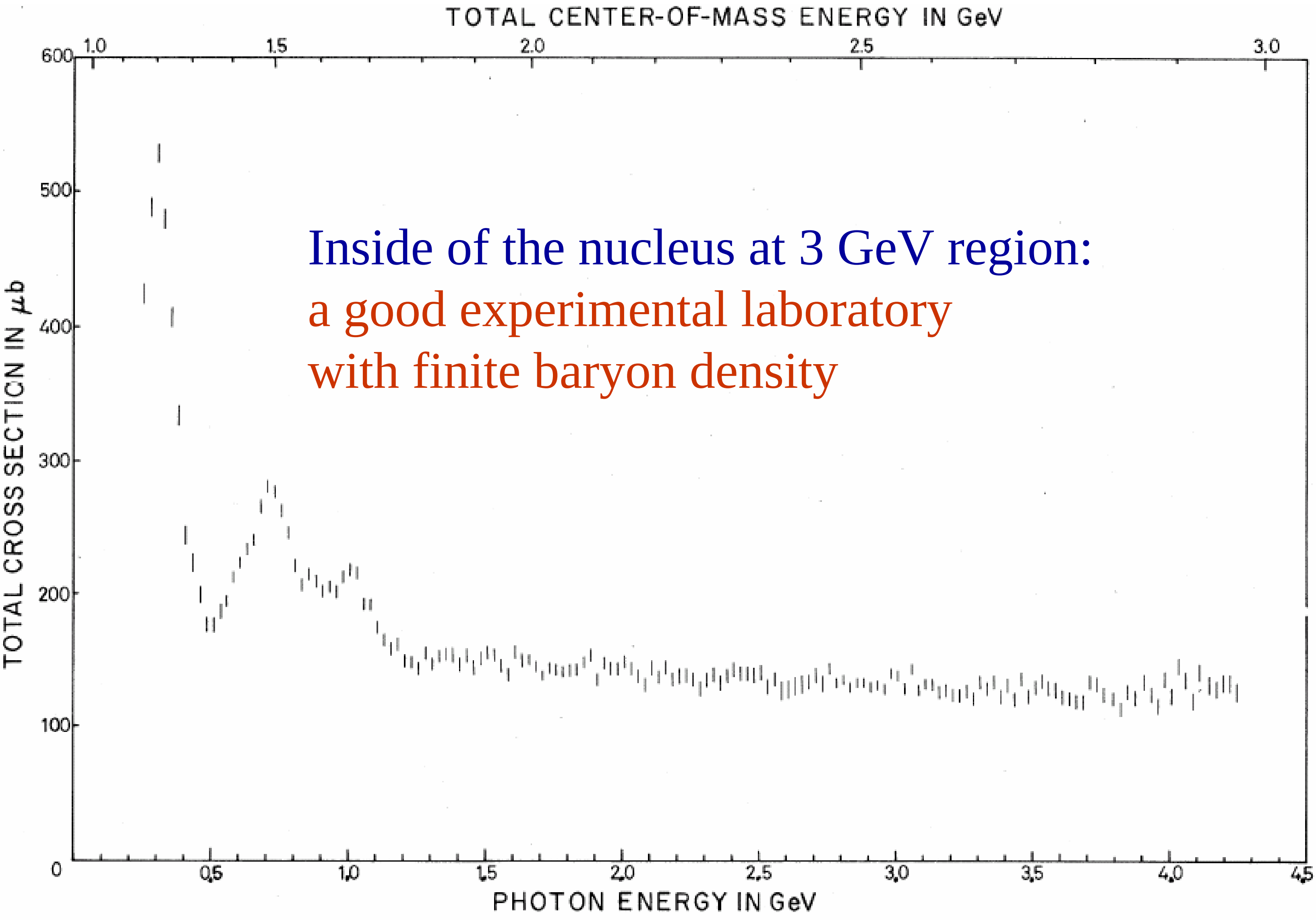

Inside of the nucleus at 3 GeV region:

a good experimental laboratory

with finite baryon density

Minimum momentum of η' in the Lab system

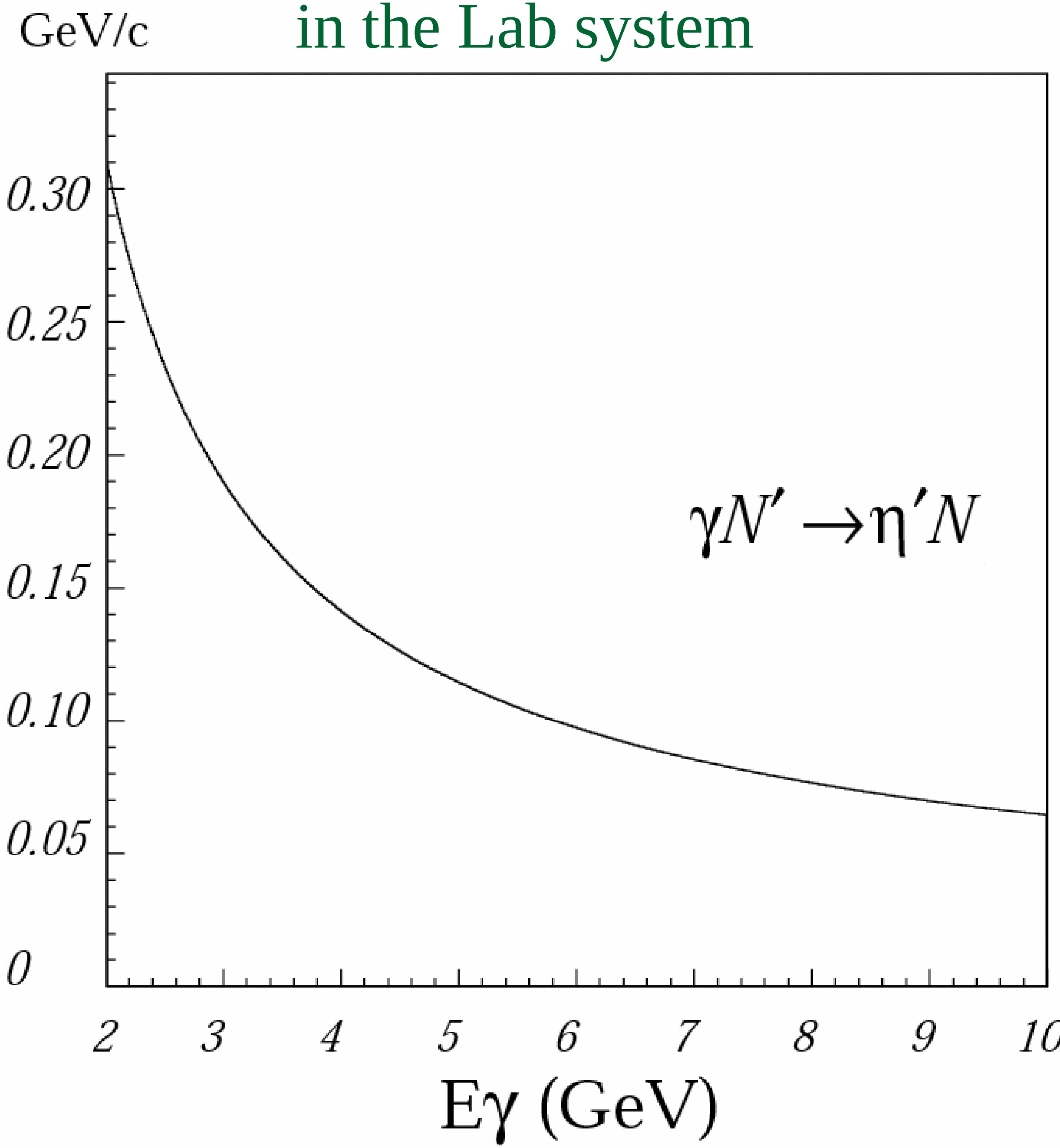

$$p_{\eta'} \leq 0.01 GeV/c$$

$$\Uparrow$$

$$\Gamma = 0.2 \text{ MeV}$$

Fermi motion may work to have p=0 η' mesons.

$$2GeV < {}^{\exists}E_{\gamma} < 10GeV$$

where $p_{\eta'} \approx 0$
if η' is bounded

=> Hirenzaki

Opening angle of 2γ in η' → γγ decay

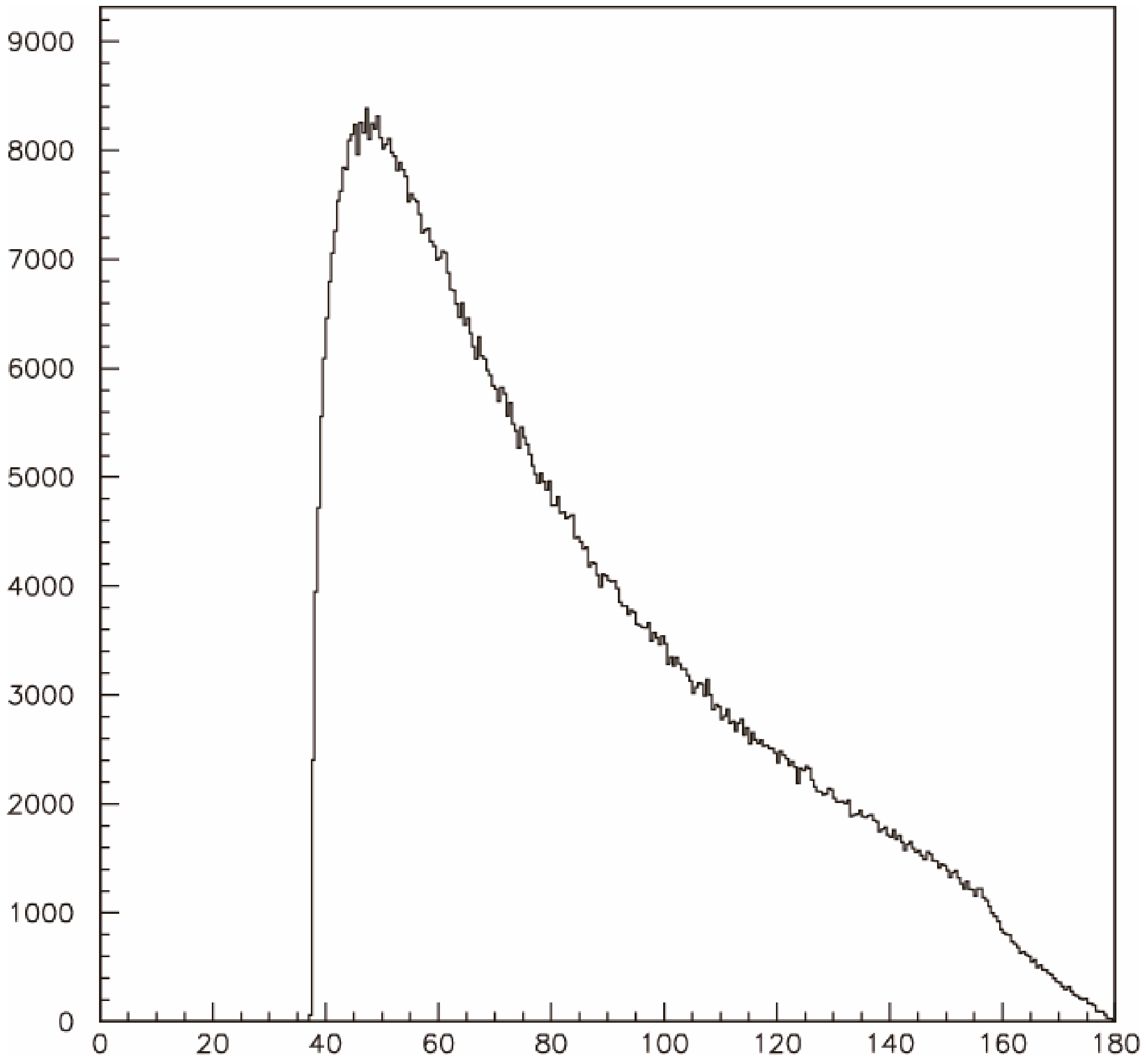

$$\gamma N' \rightarrow \eta' N$$

at Eγ = 3 GeV

Angular correlation of 2γ

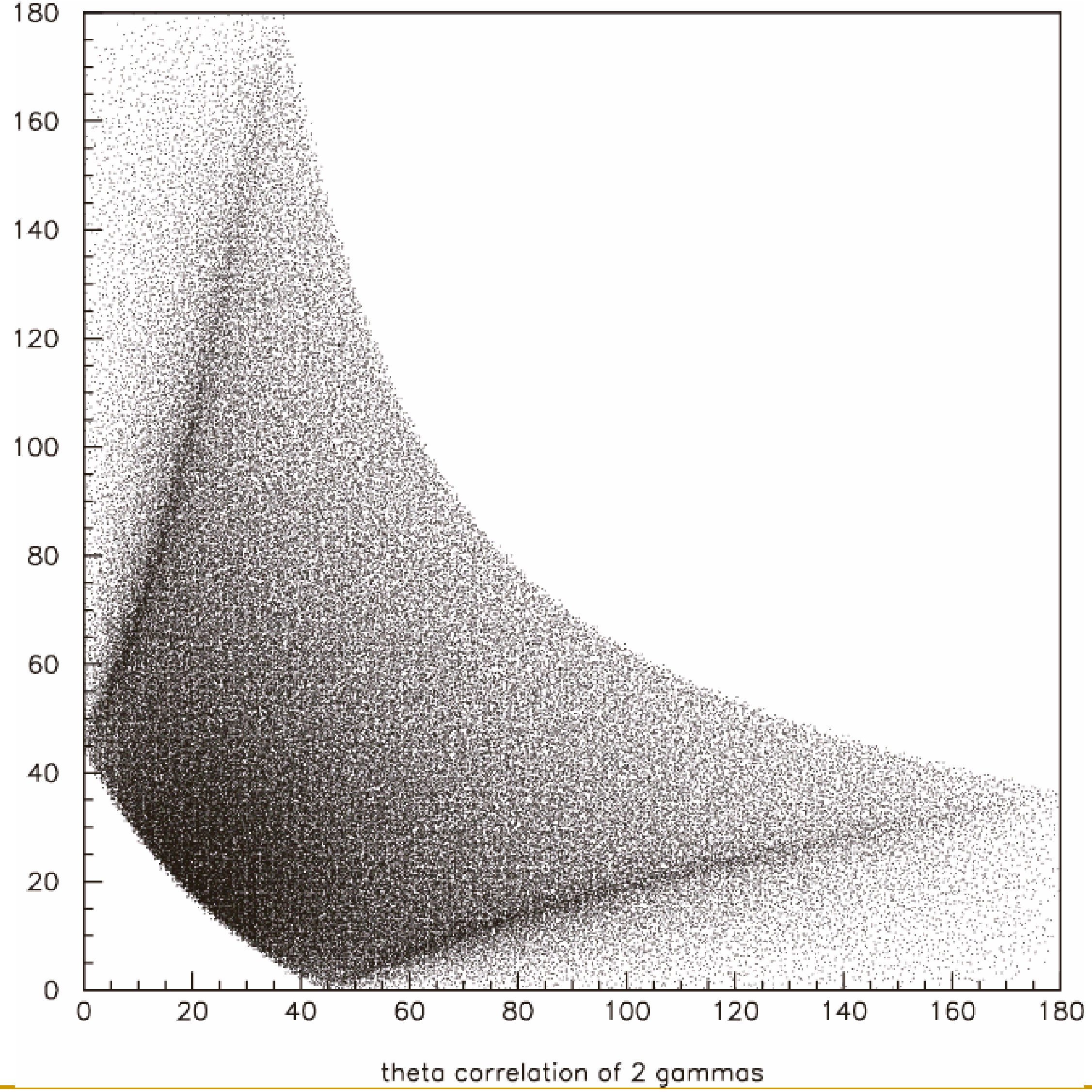

Angular distribution of γ in $\eta' \rightarrow \gamma\gamma$ decay

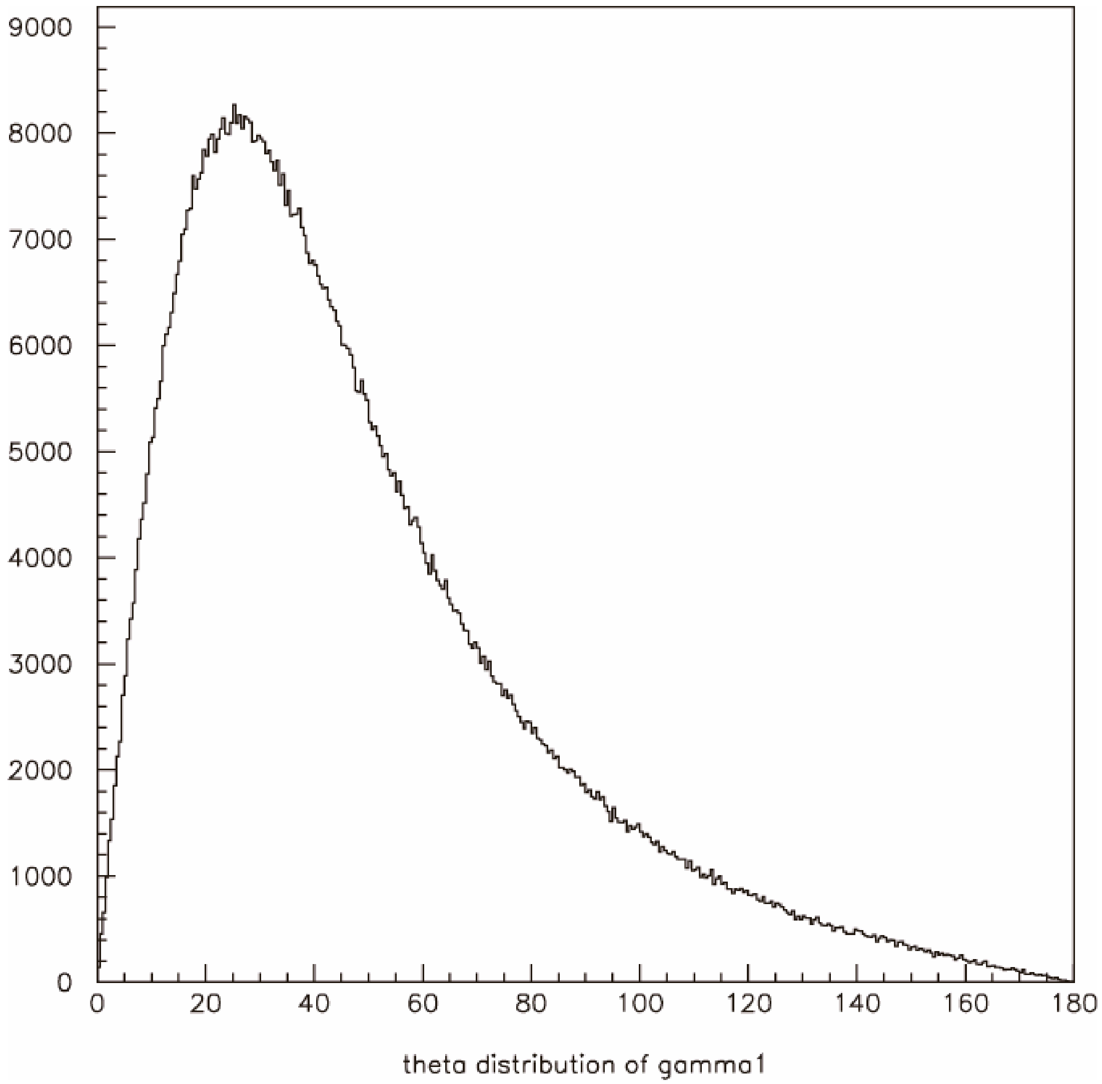

Energy distribution of γ's

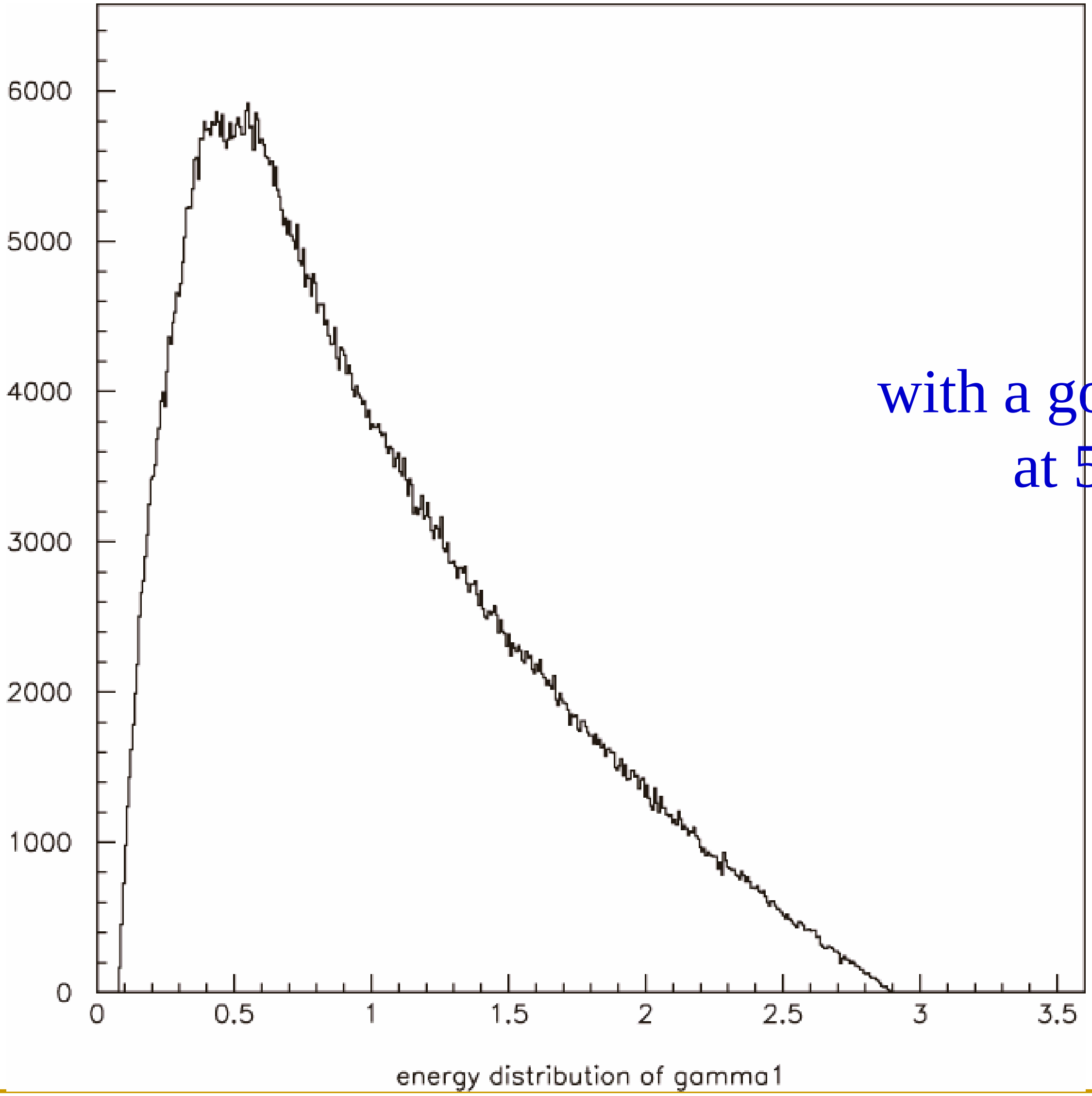

γ detectors
with a good energy resolution
at 500 MeV region

Angular distribution of η’

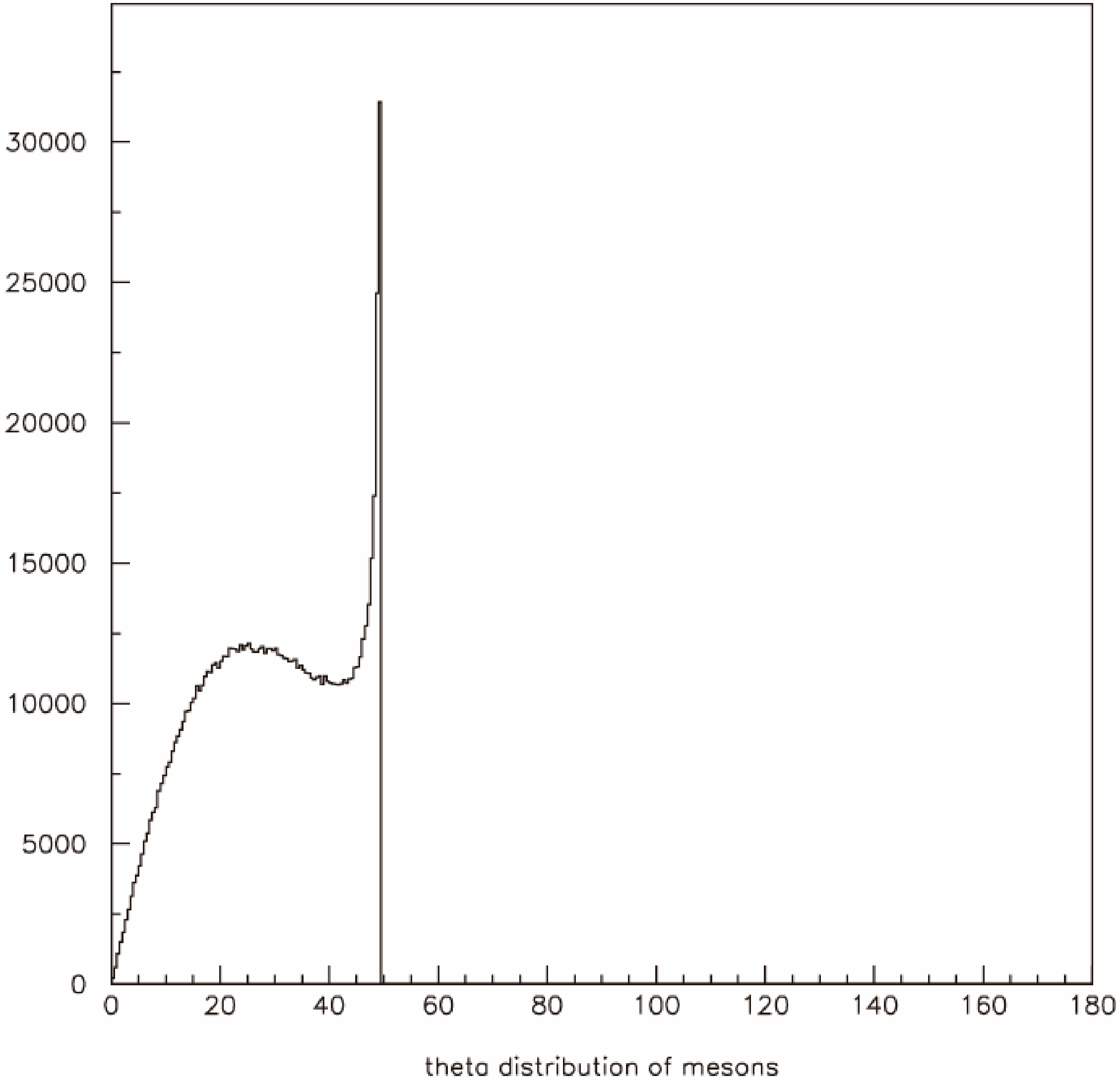

Opening angle of 2γ in η' → γγ decay

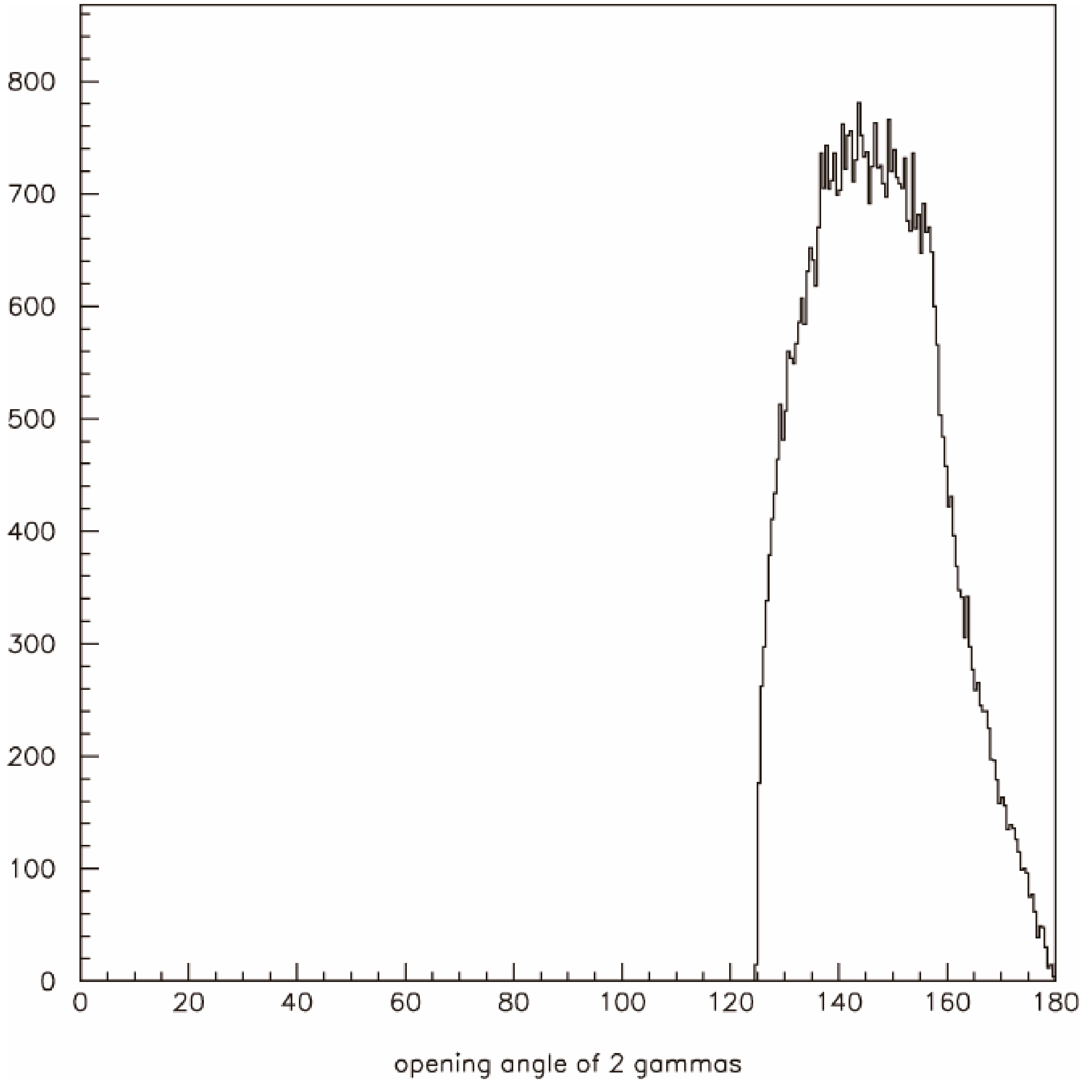

$$p_{\eta'} \leq 0.5 GeV/c$$

Angular correlation of 2γ

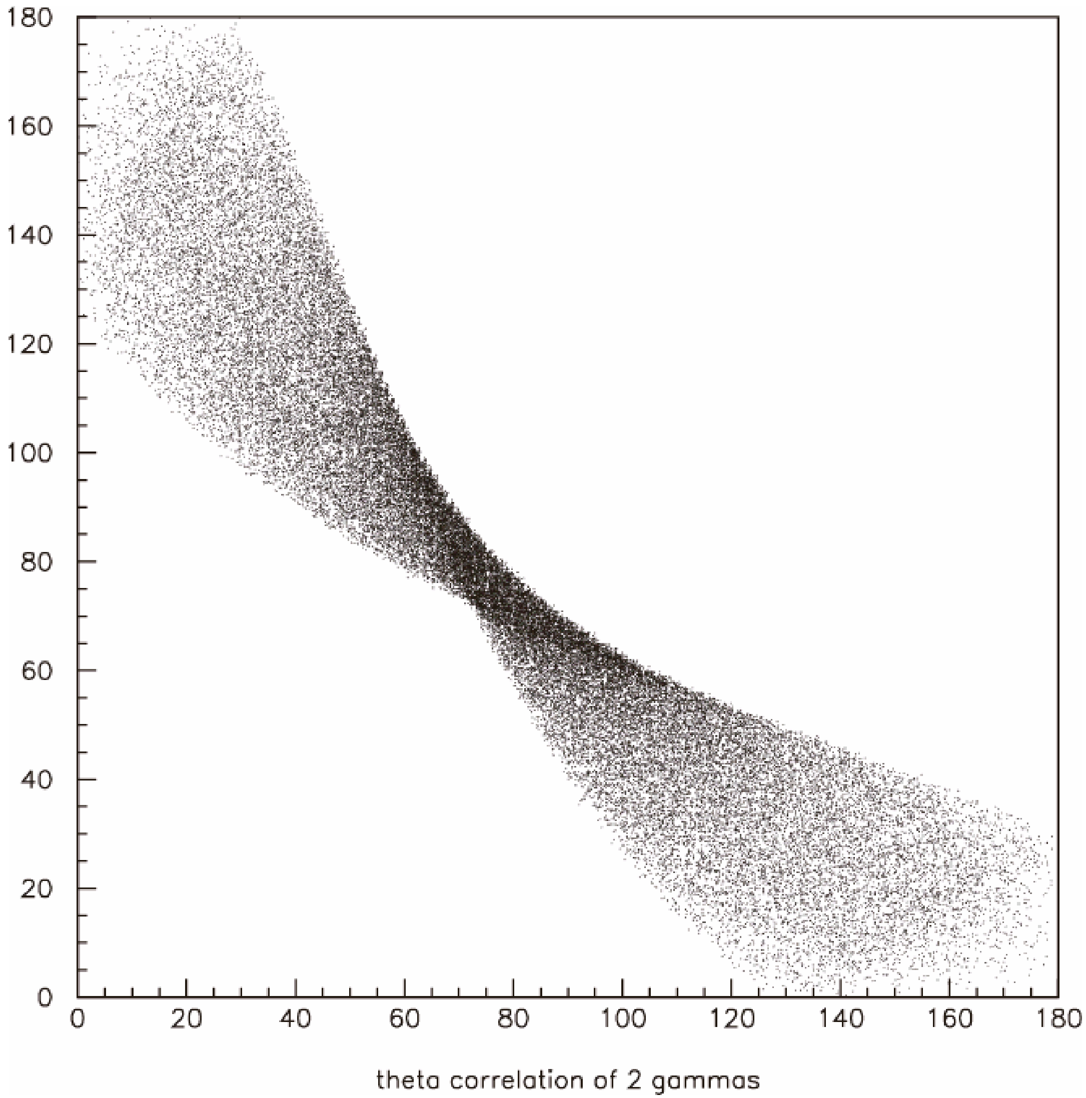

$$p_{\eta'} \leq 0.5 GeV/c$$

Angular distribution of γ's

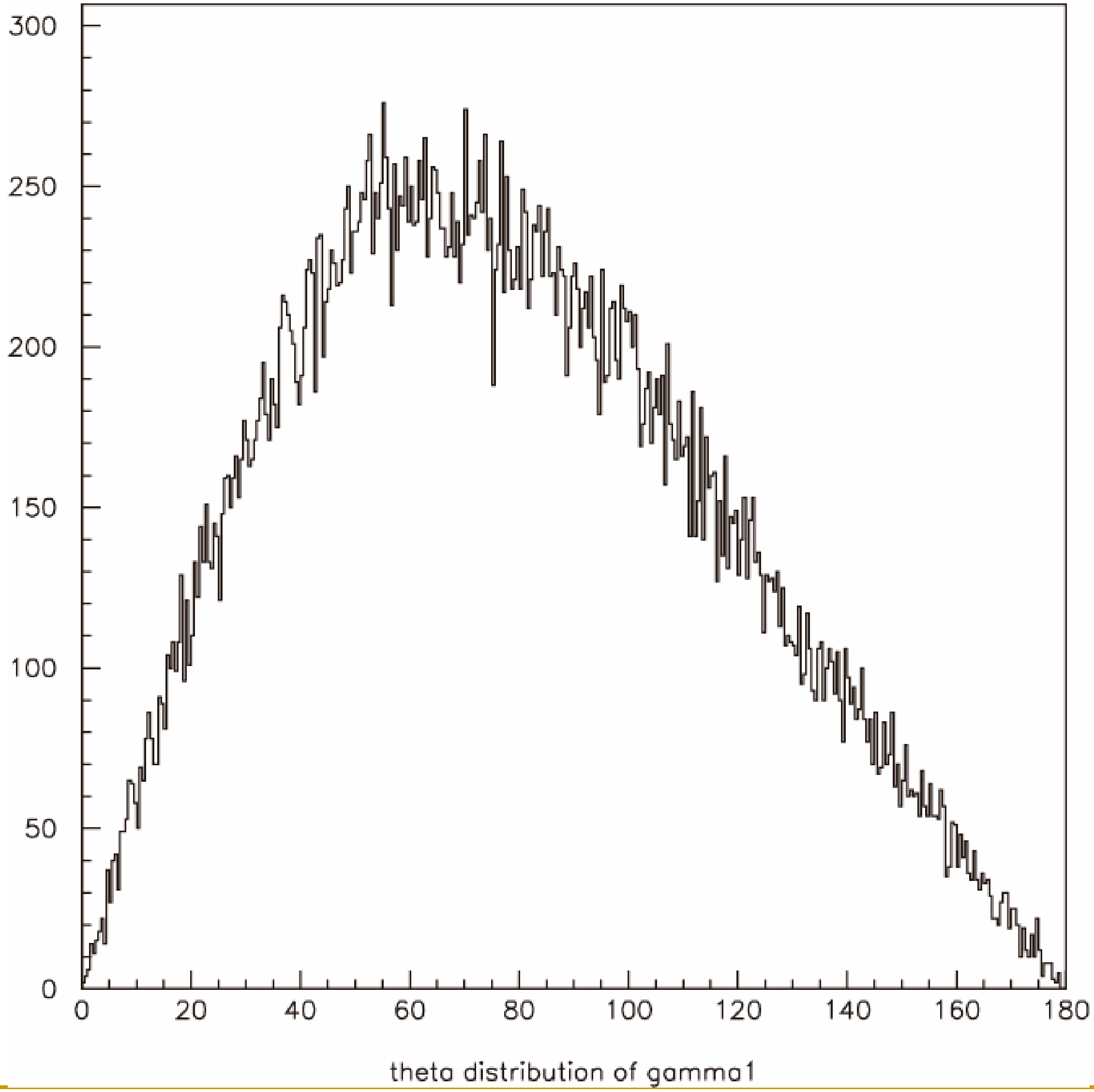

$$p_{\eta'} \leq 0.5 GeV / c$$

Energy distribution of γ's

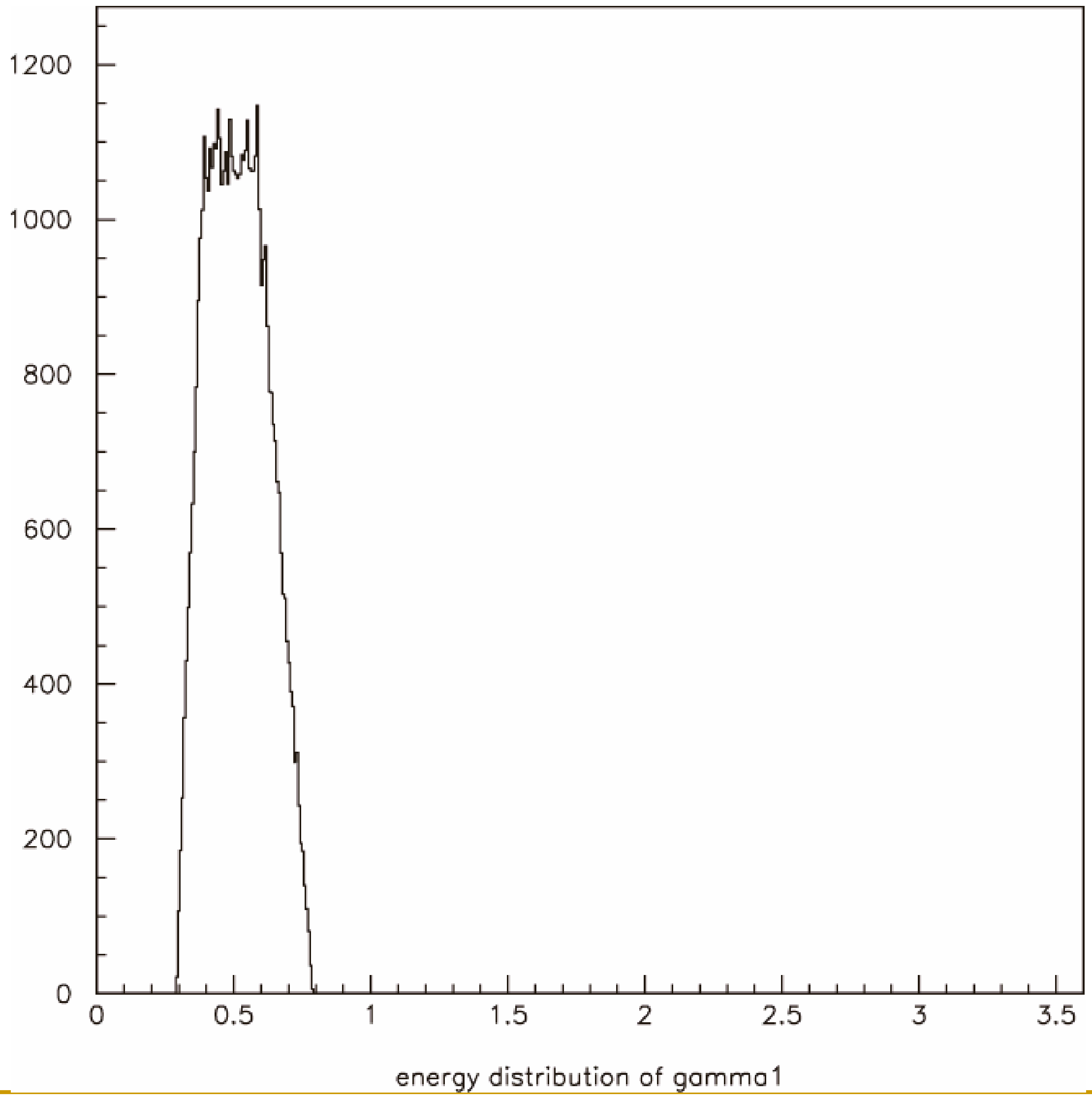

$p_{\eta'} \leq 0.5 GeV/c$

Angular distribution of outgoing nucleons

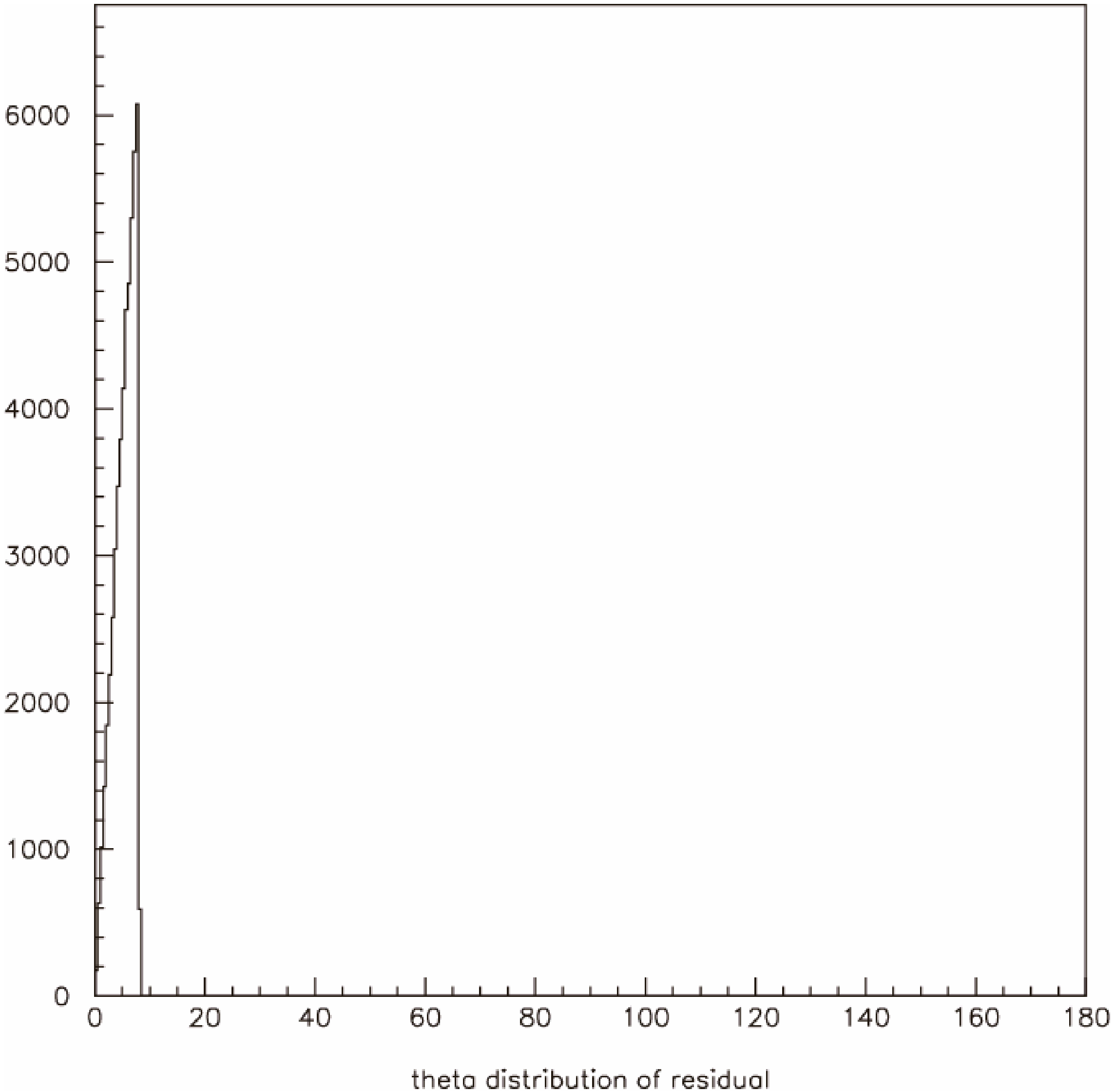

$$p_{\eta'} \leq 0.5GeV/c$$

Momentum of outgoing nucleons

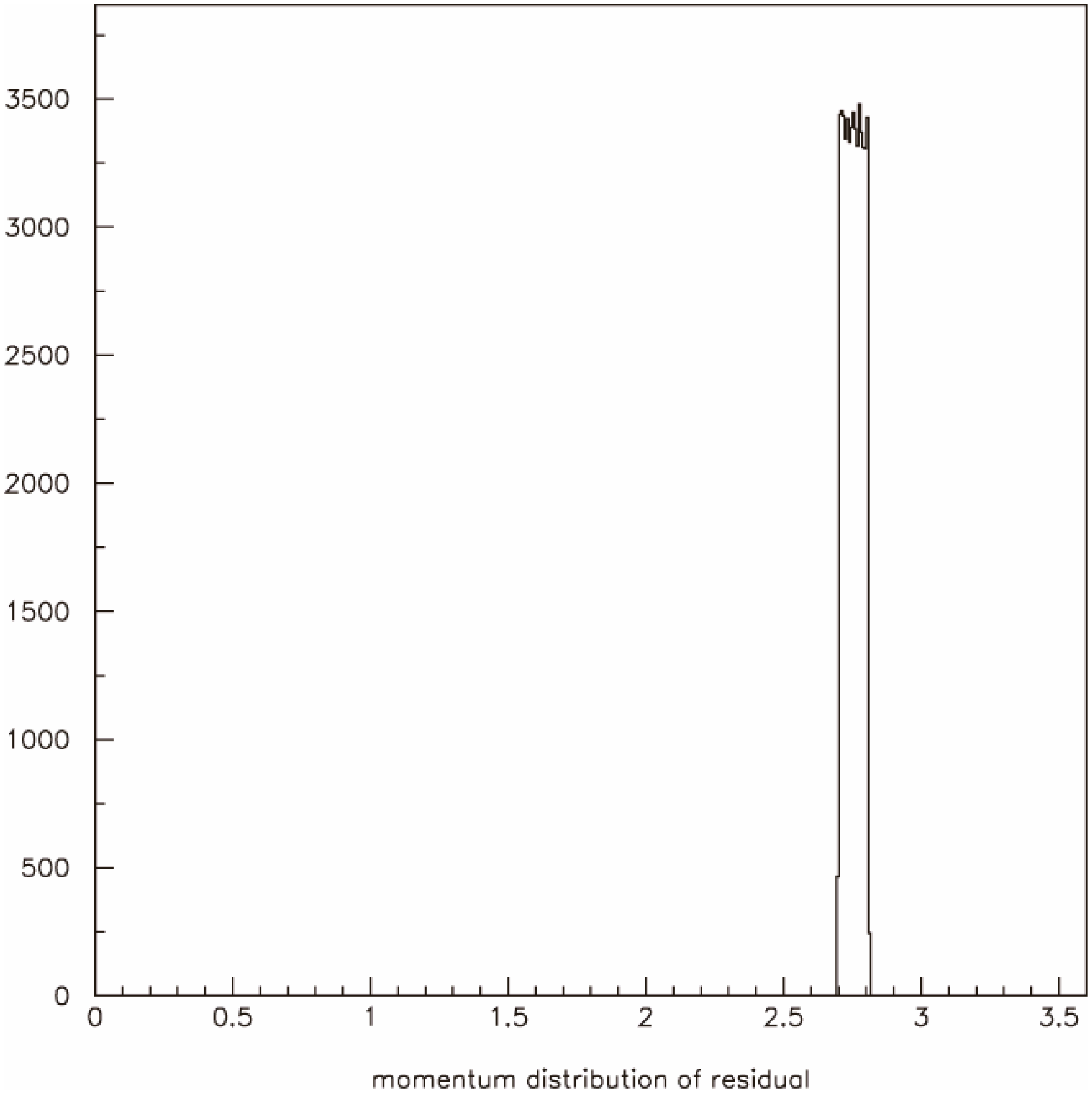

$$p_{\eta'} \leq 0.5 GeV / c$$

Schematic view of the LEPS2 facility

Backward Compton Scattering

8 GeV electron

Recoil electron (Tagging)

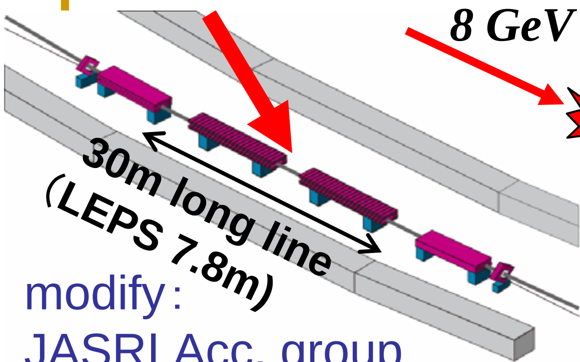

modify: JASRI Acc. group

a) SPring-8 SR ring

Laser or re-injected X-ray

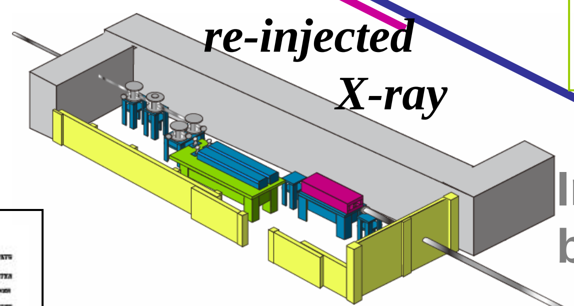

b) Laser hutch

GeV γ-ray

Inside building

Outside building

High intensity: Multi laser
LRNB
Round beam
~10 [7] photons/s (LEPS ~10 [6])

High energy: Re-injection of X-ray from undulator
(Tohoku U., JASRI)
Eγ < 7.5GeV (LEPS < 3GeV)

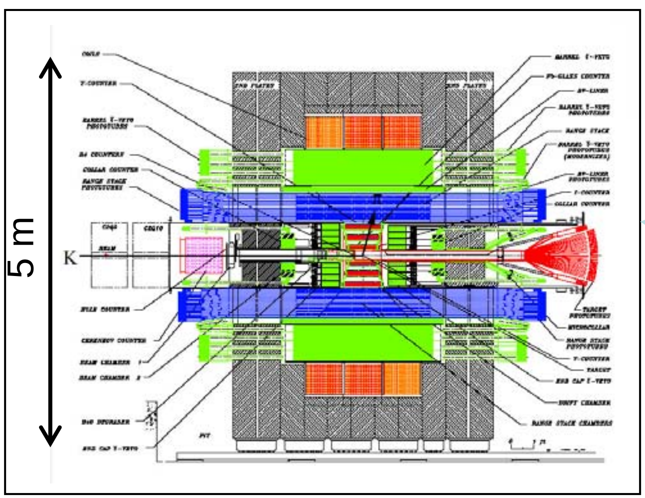

Plan to move the BNL-E949 detector to Spring-8
(helped by RIKEN)

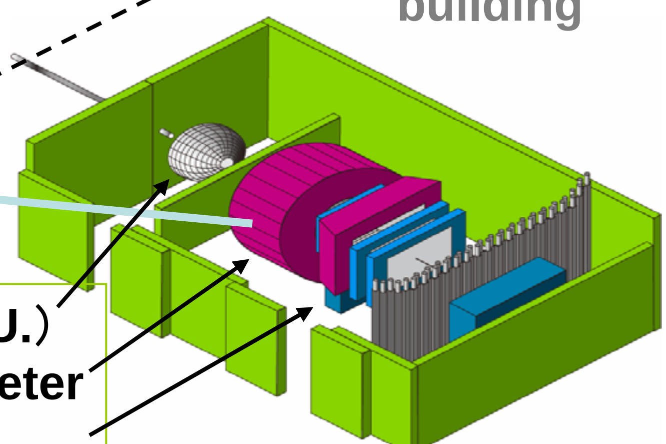

4π γ detector (Tohoku U.)
Large decay spectrometer
Forward spectrometer
New DAQ system

c) Experimental hutch

Uniqueness of new LEPS beam with 2 operational modes

- High intensity mode

  potentiality of the LEPS facility

  A tagged γ beam with the highest intensity in the world

  small low energy component =>

  small accidental coin. with untagged γ's in the beam
- High energy mode

  potentiality of the LEPS facility

  A quasi-monochromatic γ beam

  at a 7 GeV energy region

  by means of XFEL induced CBS

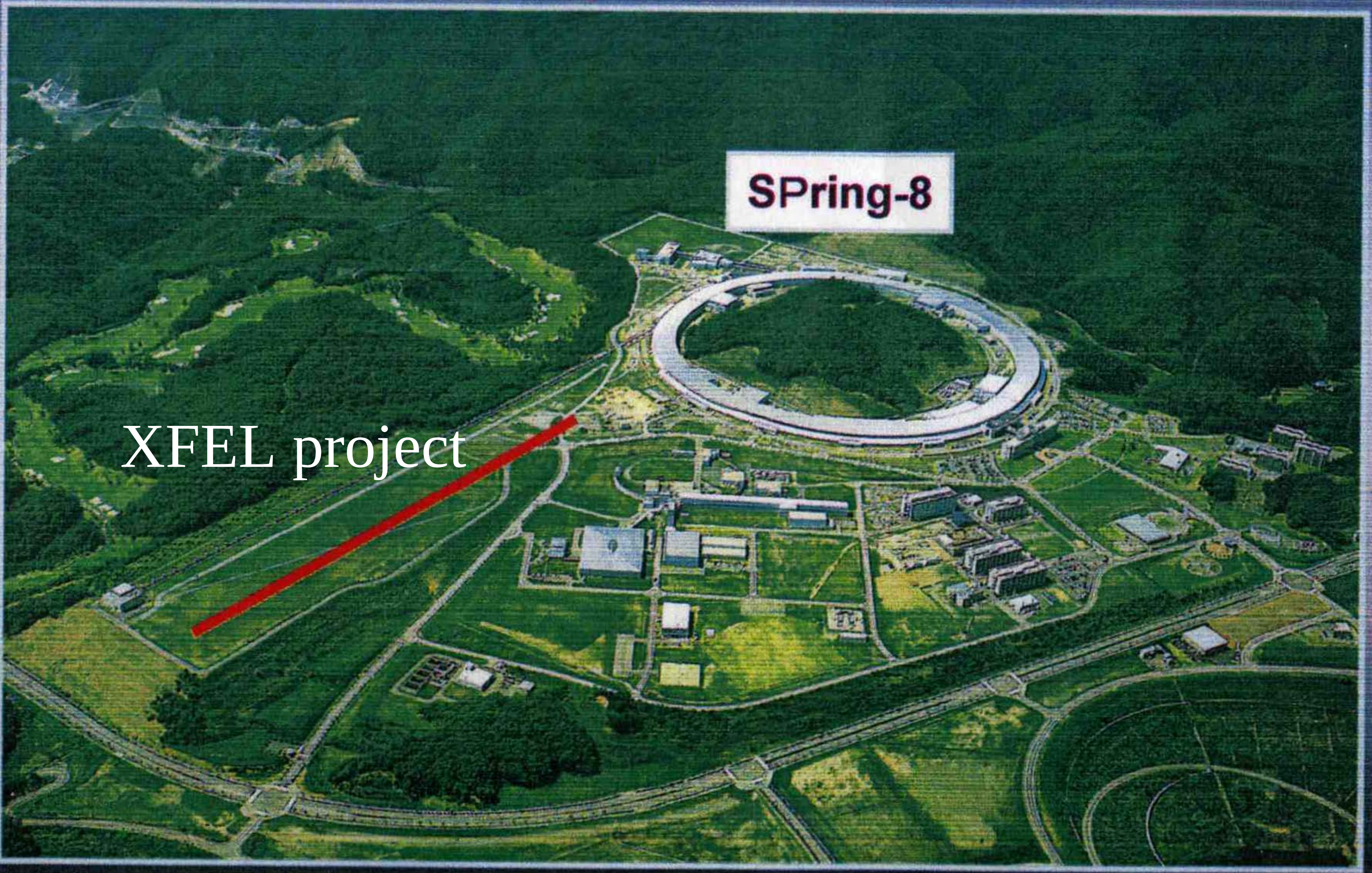
SPring-8
XFEL project

Milestone of SPring-8 X-FEL

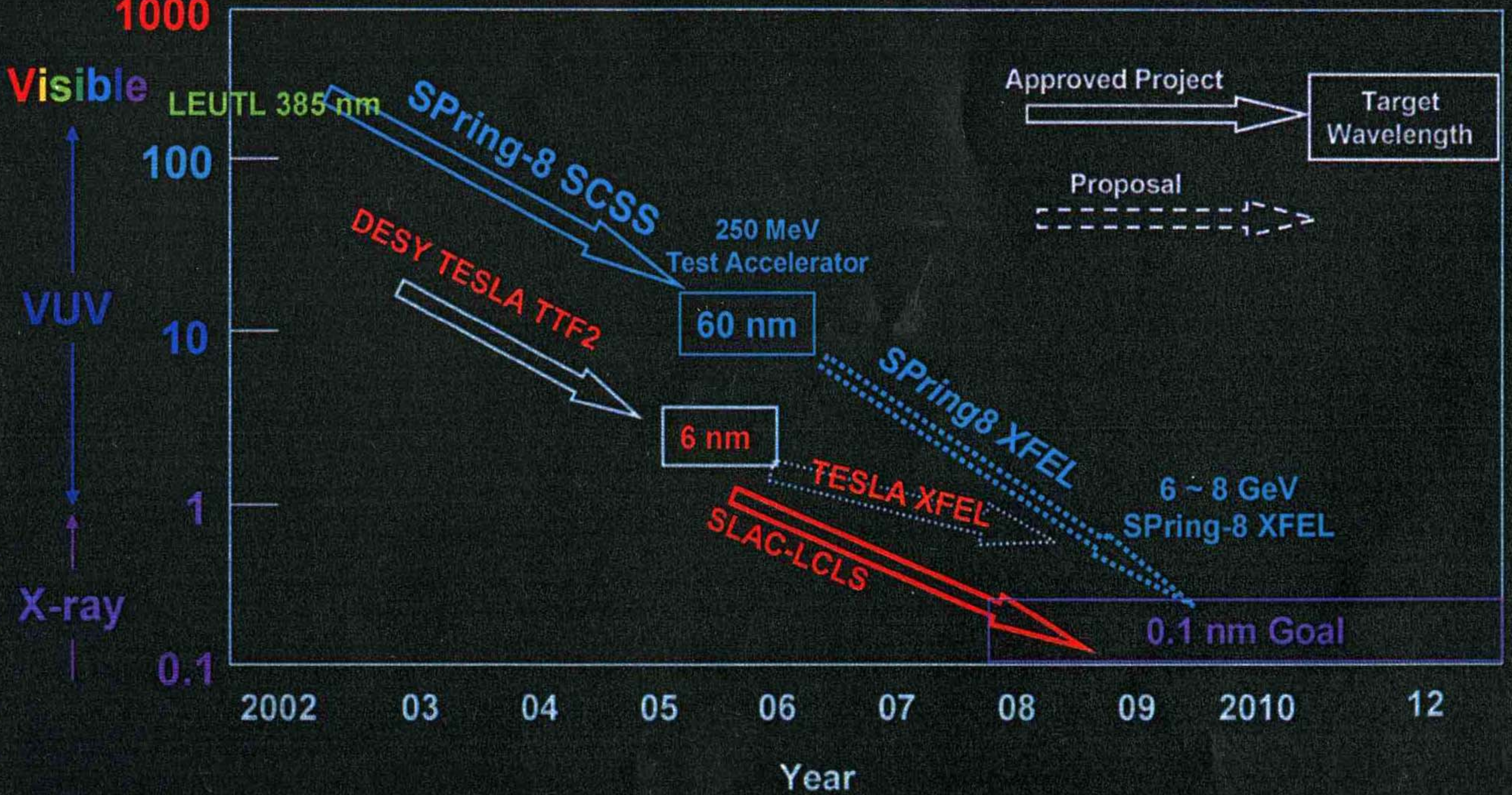

New LEPS beam (high energy mode)

High energy CBS provides a qusi-monochromatic γ beam

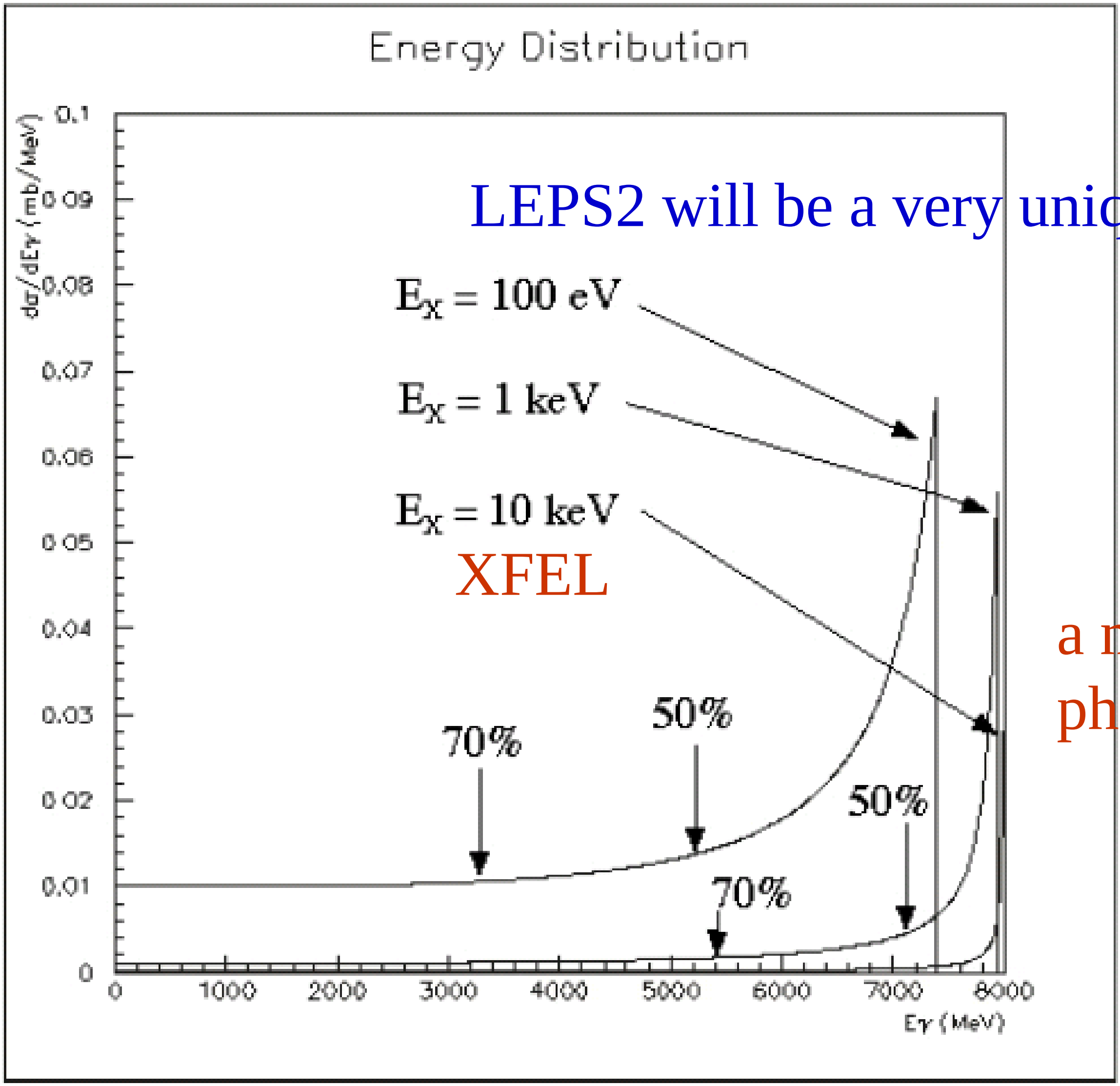

LEPS2 will be a very unique facility!

XFEL

a mono chromatic photon beam of 8GeV!